Made available by Hasselt University Library in https://documentserver.uhasselt.be

Synthesis of Highly Fluorescent All-Conjugated Alternating Donor Acceptor (Block) Copolymers via GRIM Polymerization

Peer-reviewed author version

GOVAERTS, Sanne; VERSTAPPEN, Pieter; PENXTEN, Huguette; Defour, Maxime; Van Mele, Bruno; LUTSEN, Laurence; VANDERZANDE, Dirk & MAES, Wouter

(2016) Synthesis of Highly Fluorescent All-Conjugated Alternating Donor Acceptor (Block) Copolymers via GRIM Polymerization. In: MACROMOLECULES, 49(17), p. 6411-6419.

DOI: 10.1021/acs.macromol.6b01389
Handle: http://hdl.handle.net/1942/23008

Synthesis of highly fluorescent all-conjugated alternating donor-acceptor (block) copolymers via GRIM polymerization

Sanne Govaerts,[†] Pieter Verstappen,[†] Huguette Penxten,[†] Maxime Defour,[‡] Bruno Van Mele,[‡] Laurence Lutsen,[§] Dirk Vanderzande,[†,§] Wouter Maes[,†,§]*

[†] Design & Synthesis of Organic Semiconductors (DSOS), Institute for Materials Research (IMO), Hasselt University, Agoralaan 1 – Building D, B-3590 Diepenbeek (Belgium)

[‡] Physical Chemistry and Polymer Science (FYSC), Vrije Universiteit Brussel (VUB), Pleinlaan 2, B-1050 Brussels (Belgium)

[§] IMOMEC Division, IMEC, Wetenschapspark 1, B-3590 Diepenbeek (Belgium)

Abstract

Although controlled polymerization procedures for conjugated polymers have considerable advantages with respect to molar mass and end group control, the material scope has been very limited, in particular considering block copolymers and donor-acceptor type all-conjugated polymers, imposing considerable challenges upon the synthetic polymer community. In this

work, a push-pull monomer consisting of a thiophene (donor) and a pyridine (acceptor) unit is synthesized and subsequently polymerized via Kumada catalyst-transfer polymerization using a nickel catalyst (GRIM polymerization). In this way, an alternating donor-acceptor copolymer is obtained via a chain-growth mechanism. Furthermore, an all-conjugated block copolymer containing a poly(3-hexylthiophene) block and the alternating copolymer is successfully prepared in a one-pot procedure as well. The diblock structure is confirmed by comparison of the thermal, electrochemical and spectroscopic properties of the block copolymer and its constituting polymer parts.

Introduction

Since the discovery that polyacetylene shows high conductivities after doping with halides,[1] the development of conjugated polymers has risen rapidly. Throughout the years, different classes were synthesized and investigated in several organic electronic applications, such as light-emitting diodes, transistors, photovoltaics, (bio)sensors, … .[2] One of the most studied conjugated polymers is poly(3-hexylthiophene) (P3HT), which played an important role as workhorse material to gain fundamental insights into the working principles of organic photovoltaics (OPV's).[3,4] Power conversion efficiencies up to 5% have been obtained when applying P3HT as the electron donor and [6,6]-phenyl-C_{61}-butyric acid methyl ester ($PC_{61}BM$) as the electron acceptor in polymer solar cell devices.[5] Nowadays, P3HT is outperformed by a particular class of conjugated polymers, the low bandgap donor-acceptor (D-A) alternating copolymers, which allow a more optimal harvesting of the solar spectrum.[6,7] These D-A or push-pull copolymers are generally synthesized by transition metal catalyzed polycondensation reactions, whereof the Stille and Suzuki polymerizations are the most well-known examples.[8–10] The polymerization

mechanism of these reactions is based on the formation of a new carbon-carbon bond through cross-coupling of an organohalide and an organometallic compound with the aid of a transition metal catalyst. The catalytic cycle involves three main steps, i.e. oxidative addition, transmetalation and reductive elimination. The polymerizations follow a step-growth mechanism and high molar mass polymers can only be obtained at high conversions after long reaction times. As a result, rather poor control over the polymer molar mass, dispersity and end groups is achieved, often affording ill-defined materials. On the other hand, controlled chain-growth transition metal catalyzed polycondensations allow precise control over the above-mentioned polymer characteristics and high molar mass polymers can already be obtained at low conversions. On top of that, they enable the synthesis of fully conjugated block copolymers and other advanced macromolecular structures via one-pot polymerizations. Such materials can give rise to interesting morphological structures and enhanced light absorption, beneficial for their use in for example polymer solar cells.[11–18]

In 2004, Yokozawa et al. and McCullough et al. found that the nickel-catalyzed Kumada polymerization of 2-bromo-5-chloromagnesio-3-hexylthiophene, obtained after the Grignard metathesis (GRIM) reaction of 2-bromo-3-hexyl-5-iodothiophene with an alkylmagnesium chloride reagent, followed such a controlled chain-growth mechanism.[19,20] This chain-growth mechanism results from the fact that the Ni(0) species eliminated after the reductive elimination remains associated to the growing polymer chain, whereafter it is transferred to the next C-Br bond in the same polymer chain to undergo a new oxidative addition step.[21] Since 2004, a lot of research has been done on this type of polymerization,[15,22–30] generally referred to as Kumada catalyst-transfer polymerization (KCTP), but up until now there are only two examples known wherein one has been able to synthesize an alternating copolymer in a controlled way by

performing a GRIM polymerization.[18,31] In these particular cases, a polymer consisting of two donor-type (electron rich) components was obtained. It would obviously be very interesting to extend this approach to the synthesis of low bandgap D-A alternating copolymers as this opens the door to a wide range of applications. Since both polythiophenes and polypyridines have already been synthesized in a controlled way via GRIM, we chose to create a push-pull monomer consisting of a thiophene (D) and a pyridine (A) unit.[19,20,24,32] In this work, the polymer synthesis and characterization will be discussed, as well as the tests performed to analyze the controlled character of the polymerization. Furthermore, the synthesis and characterization of an all-conjugated block copolymer, containing the alternating copolymer structure, will be elucidated.

Results and discussion

Monomer synthesis

To obtain a conjugated D-A alternating copolymer via GRIM polymerization, we opted for a precursor monomer consisting of a pyridine unit as electron deficient building block and a thiophene unit as the electron rich part. For the synthesis of the thiophene component, a Kumada coupling between 3-bromothiophene and hexylmagnesium bromide was performed, followed by bromination at the 2-position, which resulted in 2-bromo-3-hexylthiophene (**1**) (Scheme 1). The pyridine unit on the other hand was synthesized by selectively exchanging the bromine at the 5-position of 2,5-dibromopyridine with iodine, affording 2-bromo-5-iodopyridine (**2**). Afterwards, the pyridine unit was coupled onto the thiophene through a Negishi coupling, whereby 2-bromo-5-(3'-hexylthiophen-2'-yl)pyridine (**3**) was obtained. The 'para' coupling pattern is important to make sure that the final polymer is fully conjugated. In a last step, compound **3** was iodinated at

the 5-position of the thiophene unit to end up with 2-bromo-5-(3'-hexyl-5'-iodothiophen-2'-yl)pyridine (**4**) as the precursor monomer.

Scheme 1. Precursor monomer synthesis.

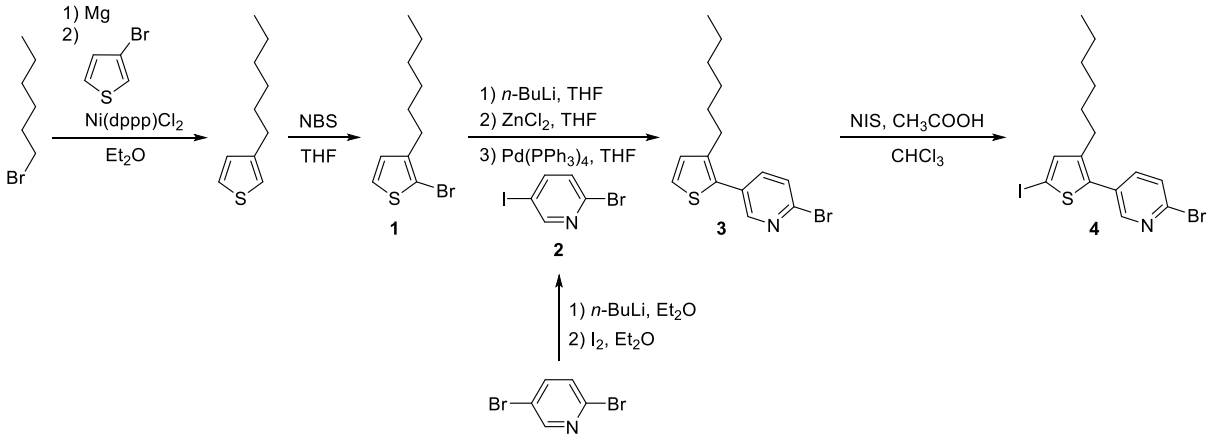

Once the precursor monomer **4** was obtained, the active monomer **M1** could be formed via a GRIM reaction (Scheme 2). This was done prior to the polymerization by adding 1.0 equivalents of *i*-PrMgCl.LiCl to **4** in dry THF at 0 °C, whereby a concentration of 0.1 M was maintained, and letting it react for 1 h. During the GRIM reaction, the iodine end group of **4** was selectively replaced by a magnesium chloride group and the bromine end group remained intact as confirmed by a water quenching test and subsequent ^{1}H NMR analysis. Moreover, complete conversion of the precursor monomer **4** to the active monomer **M1** was observed. The above conditions for the GRIM reaction (0 °C, 1 h and [**M1**] = 0.1 M) were therefore used for all polymerizations described below.

Scheme 2. Synthesis of the **P(3HT-*alt*-P)** copolymer via GRIM polymerization.

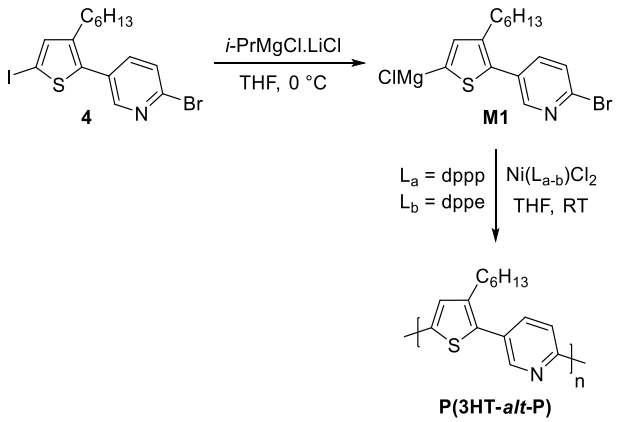

Alternating copolymer synthesis

Since both polypyridines and polythiophenes have been prepared before in a controlled way via KCTP using Ni(dppp)Cl_2 as the catalyst,[19,20,24] these conditions were also used for the synthesis of the targeted alternating polymer poly[(3-hexylthiophene-5,2-diyl)-*alt*-(pyridine-5,2-diyl)] **P(3HT-*alt*-P)** (Scheme 2). A first polymerization test was performed by adding the *in situ* formed monomer **M1** to 1 mol% of Ni(dppp)Cl_2 in dry THF ([**M1**] = 0.075 M) at RT (Table 1, Test 1). Aliquots of the polymerization mixture were taken at different time intervals and analyzed by gel permeation chromatography (GPC) to determine the molar mass (M_n), conversion (p) and polydispersity (PDI). These values are important to gain more insight into the polymerization mechanism, for instance by plotting M_n versus p and ln([**M1**]$_0$/[**M1**]) versus time. If both of these plots show a linear correlation, the polymerization proceeds via a controlled chain-growth mechanism.[19,26,33] From the GPC results, however, no clear plots could be obtained since the molar mass of the polymer was already ~20 000 g/mol after 1 minute and did not increase significantly thereafter (Figure S7, Supporting Information). So, to be able to investigate the polymerization mechanism, the polymerization speed had to be decreased. This was done by lowering the concentration and temperature during different polymerization tests. Nevertheless,

the same result was obtained (Table 1, Tests 2-7). When the concentration became too low, no polymer was formed at all (Table 1, Test 8). Then, another polymerization test was performed with a different nickel catalyst, Ni(dppe)Cl_2, under the same conditions as the initial polymerization test (Table 1, Test 9). Again, a molar mass of ~20 000 g/mol was obtained after 1 minute, which did not increase substantially afterwards (Figure S8, Supporting Information). From all of these polymerization tests, it can be concluded that the polymerization does not proceed in a controlled way, since the polymer chains do not continue to grow any further once a M_n of ~20 000 g/mol is achieved, although there is still monomer present in the polymerization mixture.

Table 1. GRIM polymerization of **M1** under different reaction conditions.

Test	Catalyst (1 mol%)	Temperature	[**M1**] (M)	M_n x 10^4 (g/mol)	PDI
1	Ni(dppp)Cl_2	RT	0.075	2.6[a]	1.28
2	Ni(dppp)Cl_2	0 °C	0.075	2.1	1.29
3	Ni(dppp)Cl_2	RT	0.03	1.7	1.40
4	Ni(dppp)Cl_2	0 °C	0.01	1.8	1.37
5	Ni(dppp)Cl_2	RT	0.0075	1.9	1.19
6	Ni(dppp)Cl_2	RT	0.005	2.3	1.23
7	Ni(dppp)Cl_2	RT	0.0045	2.2	1.36
8	Ni(dppp)Cl_2	RT	0.002	/	/
9	Ni(dppe)Cl_2	RT	0.075	2.3[a]	1.29

[a] After purification by Soxhlet extraction.

This observation motivated further analysis to obtain more insights in the polymerization mechanism. To this extent, new polymerization tests were performed whereby each time the same amount of **M1** (0.20 mmol) was used under the same reactions conditions ([**M1**] = 0.05 M and RT) and only the amount of Ni(dppp)Cl_2 catalyst was altered (1, 2.5, 5 and 10 mol%). The results of those tests are depicted in Figure 1. It is clear that for all different catalyst amounts roughly the same M_n values (~18 000 g/mol) were obtained. The same can be said for the polydispersities, which all lie around 1.4. This confirms our previous assumption that the

polymerization does not happen in a controlled way. On the other hand, the low polydispersities and high molar masses at low conversions point out that the polymerization follows a chain-growth mechanism. It can be concluded that the polymerization of **P(3HT-*alt*-P)** proceeds via a non-controlled chain-growth mechanism, whereby the growing polymer chains are terminated once they have reached a M_n value of ~20 000 g/mol.

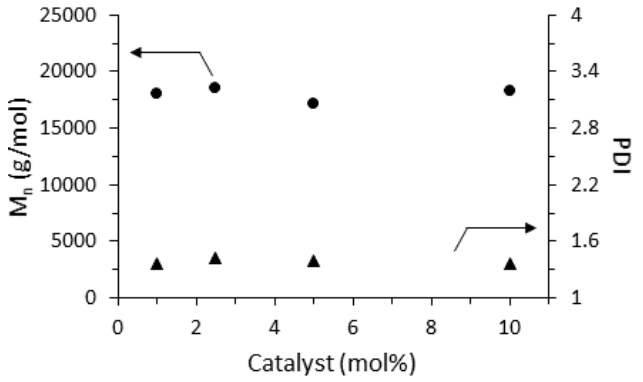

Figure 1. Relation between the amount of catalyst used and the resulting molar mass and polydispersity.

Since these termination reactions have a strong influence on the polymerization characteristics of **P(3HT-*alt*-P)**, it would be interesting to reveal which type of termination reaction is dominant. In case of KCTP polymerization, the association of the catalyst to the growing polymer chain after reductive elimination is essential to obtain the controlled chain-growth character. This means that there are two types of termination reactions possible, i.e. disproportionation and dissociation (Scheme 3).[30]

Scheme 3. Catalytic cycle of a GRIM polymerization with its possible termination reactions.[30]

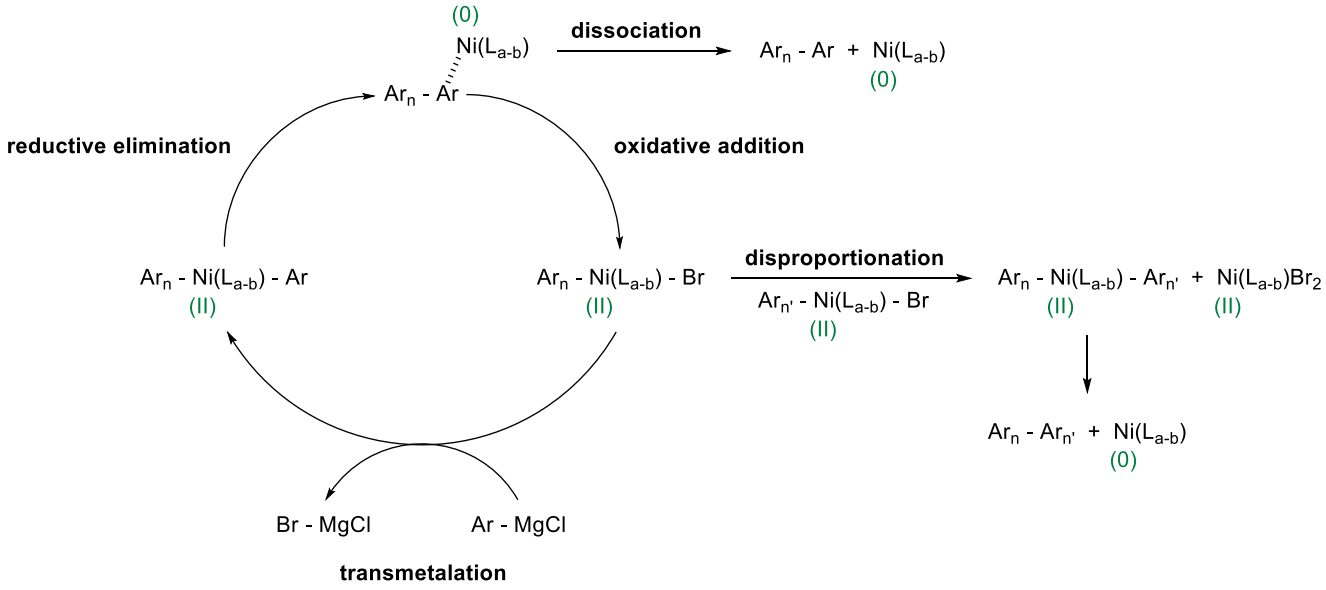

When disproportionation is the dominant termination reaction, it goes in competition with the transmetalation step, which results into a degree of polymerization (X_n) that is defined by the ratio of the rate of transmetalation (R_{TM}) and the rate of disproportionation (R_{disp}). If, however, dissociation is the dominant termination reaction, X_n is determined by the ratio of the rate of oxidative addition (R_{OA}) and the rate of dissociation (R_{diss}). This results into the following equations:

- If disproportionation is dominant:

$$X_n = \frac{R_{TM}}{R_{disp}} = \frac{k_{TM}[In]_0[M]_0}{k_{disp}[In]_0[In]_0} \quad (1)$$

- If dissociation is dominant:

$$X_n = \frac{R_{OA}}{R_{diss}} = \frac{k_{OA}[In]_0}{k_{diss}[In]_0} \quad (2)$$

whereby $[In]_0$ is the initial initiator concentration, $[M]_0$ is the initial monomer concentration and k_{TM}, k_{disp}, k_{OA} and k_{diss} are the rate constants for transmetalation, disproportionation, oxidative addition and dissociation, respectively.[30] Out of these equations, it can be deduced that if

disproportionation is dominant, the degree of polymerization (and hence the molar mass) is dependent of $[M]_0/[In]_0$. On the contrary, when dissociation is the dominant termination reaction, X_n is independent of $[M]_0/[In]_0$. All polymerization tests, wherein first only $[M]_0$ was altered (Table 1) and afterwards only $[In]_0$ was varied (Figure 1), clearly show that the molar mass is independent of $[M]_0/[In]_0$. This points out that dissociation is most likely the dominant termination reaction in our non-controlled chain-growth polymerization of **P(3HT-*alt*-P)**. These results are in agreement with previous findings that difficulties arise in the KCTP polymerizations of n-type monomers due to the fact that they have a weaker π-donor ability to stabilize the polymer-nickel complex after reductive elimination, leading to shorter lifetimes of the growing polymer chains.[34] This could explain why no polymer is formed at all when the concentrations are too low (Table 1, Test 8), because in this case it takes too long to find another monomer unit in the vicinity to react with, causing the Ni catalyst to dissociate from the growing entity.

Another way to obtain more insights into the polymerization mechanism is to investigate the end groups of the polymer chains by performing MALDI-TOF (matrix-assisted laser desorption ionization - time of flight) mass spectrometry measurements. From literature, it is known that only polymer chains with Br/H end groups are formed in case of a controlled chain-growth mechanism.[35] When termination reactions occur, however, also polymer chains with Br/Br or H/H end groups are formed.[36] In our case, dissociation seems to be the dominant termination reaction, which results in polymer chains with Br/Br end groups. The MALDI-TOF spectrum of **P(3HT-*alt*-P)** (Table 1, Test 9) is displayed in Figure S9 (Supporting Information). It is clear that there are two main distributions present. The smaller signals correspond to polymer chains with Br/H end groups, whereas the most intense signals can be attributed to polymer chains with

Br/Br end groups. These observations confirm the non-controlled chain-growth character of the GRIM polymerization of **P(3HT-*alt*-P)**, due to dissociation of the nickel catalyst.

Block copolymer synthesis

For the synthesis of the block copolymer we decided to start with an *in situ* formed **P3HT** block that is used as macro-initiator for the polymerization of **P(3HT-*alt*-P)** as the second block (Scheme 4). This was done by first performing a GRIM reaction on 2,5-dibromo-3-hexylthiophene with one equivalent of *i*-PrMgCl.LiCl at 0 °C for 1 h, resulting in 2-bromo-5-chloromagnesio-3-hexylthiophene as active monomer **M2**. Then, this monomer was polymerized with 0.65 mol% of Ni(dppp)Cl_2 at RT ([**M2**] = 0.075 M). After a polymerization time of 15 min, half of the polymerization mixture was cannulated to another flask and quenched with a MeOH/HCl mixture, which resulted into the **P3HT** reference homopolymer. To the other half of the polymerization mixture, the *in situ* prepared active monomer **M1** was added to create the second block. After a polymerization time of 30 min at RT the polymerization mixture was quenched with water, yielding poly{[3-hexylthiophene-5,2-diyl]-*block*-[(3-hexylthiophene-5,2-diyl)-*alt*-(pyridine-5,2-diyl)]} **P3HT-*b*-P(3HT-*alt*-P)**. Both the **P3HT** homopolymer and the **P3HT-*b*-P(3HT-*alt*-P)** block copolymer were purified by Soxhlet extraction with MeOH, acetone, hexane and chloroform (dissolving the polymer), respectively. All polymeric material was found to be soluble in THF and $CHCl_3$.

Scheme 4. Synthesis of the **P3HT-*b*-P(3HT-*alt*-P)** copolymer.

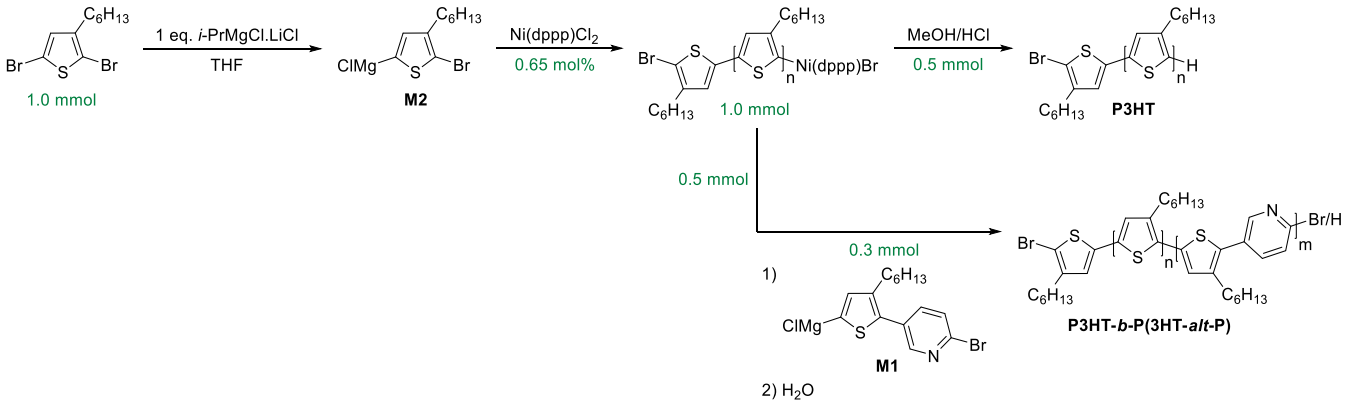

A first test performed to check whether a block copolymer was indeed formed, was the analysis of both **P3HT** and **P3HT-*b*-P(3HT-*alt*-P)** by GPC. The resulting GPC profiles clearly show a shift to higher M_n values, while maintaining a unimodal curve (Figure 2). The **P3HT** homopolymer was characterized by a M_n value of 23 000 g/mol and a PDI of 1.15, while the **P3HT-*b*-P(3HT-*alt*-P)** block copolymer showed a M_n value of 41 000 g/mol and a PDI of 1.37. These M_n values correspond reasonably well to what was expected. By using 0.65 mol% of $Ni(dppp)Cl_2$, a M_n value of ~25 000 g/mol (~150 monomer units of 166 g/mol) was foreseen for **P3HT**. This value was targeted since we aimed at a doubling of the molar mass for the block copolymer and it was already established that the **P(3HT-*alt*-P)** polymer chains always grew till a length of ~20 000 g/mol.

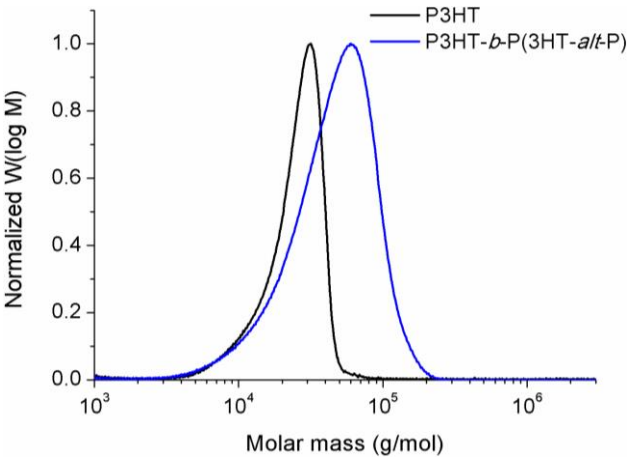

Figure 2. GPC profiles of the **P3HT** homopolymer and the **P3HT-*b*-P(3HT-*alt*-P)** copolymer.

The fact that a unimodal curve was obtained for the block copolymer indicates that the 'living' **P3HT** polymer chains grew further to end up with **P3HT-*b*-P(3HT-*alt*-P)** chains. This could be confirmed by studying both materials via ^{1}H NMR spectroscopy. First, the α-CH_2 region of the hexyl side chains of the **P3HT** homopolymer was analyzed (Figure 3a). Three different triplets were distinguished, whereof the biggest signal (**a**) at 2.80 ppm could be ascribed to the α-CH_2 protons of the internal **P3HT** units, whereas the two smaller signals correspond to the α-CH_2 protons of the two external thiophene units with a hydrogen end group (signal **b** at 2.62 ppm) and a bromine end group (signal **c** at 2.58 ppm), according to McCullough *et al.*[37] Then, an overlay of the ^{1}H NMR spectra of the α-CH_2 regions of **P3HT** and **P3HT-*b*-P(3HT-*alt*-P)** was studied (Figure 3b). From this overlay, it is clear that signal **b** of **P3HT** disappeared (or at least largely reduced), suggesting that (most of) the **P3HT** polymer chains reacted further to give the block copolymer. Besides this, another signal (**d** at 2.75 ppm) appeared in the spectrum of the **P3HT-*b*-P(3HT-*alt*-P)** copolymer, which could be ascribed to the α-CH_2 protons of the hexyl side chains of the second block.

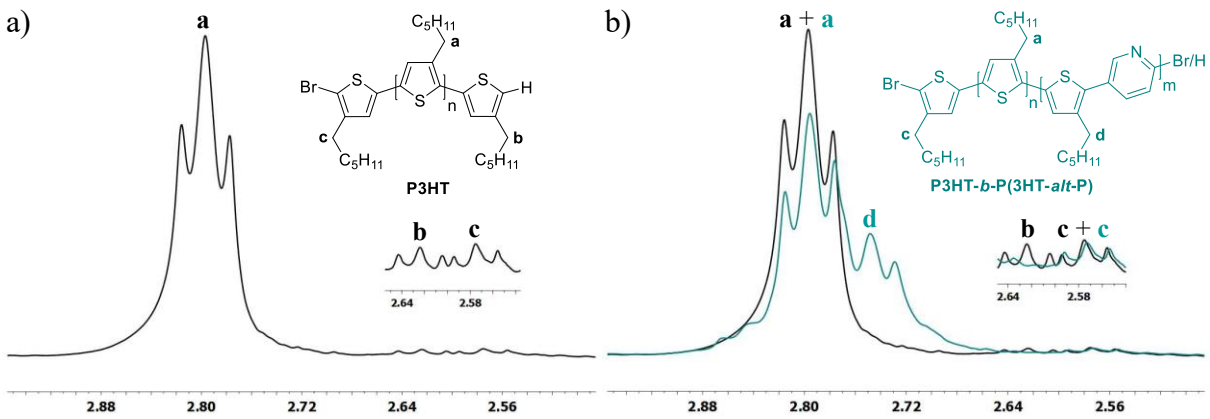

Figure 3. a) ^{1}H NMR spectrum of the α-CH_2 region of **P3HT**; b) Overlay of the ^{1}H NMR spectra of the α-CH_2 regions of **P3HT** and **P3HT-*b*-P(3HT-*alt*-P)**.

As we cannot exclude from the NMR analysis that minor amounts of non-chain-extended **P3HT** are still present in the block copolymer sample, as might be inferred from the tailing at the low molar mass side of the GPC profile (Figure 2), preparative GPC was used to remove the low-molar mass part. The two separate fractions obtained were then analyzed by GPC and ^{1}H NMR spectroscopy, from which it can be concluded that ~3−4% of **P3HT** is present in the block copolymer (Figure S10-12, Supporting Information).

Also the other order of monomer addition was investigated (starting from **P(3HT-*alt*-P)**), but in this case no block copolymer was formed. This is not surprising since it was already established that the growing **P(3HT-*alt*-P)** polymer chains are terminated once they have reached a M_n value of ~20 000 g/mol after just a few minutes. This observation, together with the successful block copolymerization starting from a **P3HT** block, further strengthens our hypothesis that the **P(3HT-*alt*-P)** copolymer is formed via a non-controlled chain-growth polymerization.

Thermal, electrochemical and optical characterization

First of all, the thermal properties of the synthesized materials were analyzed by performing rapid heat-cool calorimetry (RHC) measurements on the **P(3HT-*alt*-P)** copolymer, the **P3HT** homopolymer and the **P3HT-*b*-P(3HT-*alt*-P)** copolymer. Also a blend of **P3HT** and **P(3HT-*alt*-P)** was made for comparison and characterized in the same way. This blend was created by mixing 40% of **P(3HT-*alt*-P)** with 60% of **P3HT**, approaching the constitution of the block copolymer (based on integration of the ^{1}H NMR spectrum of **P3HT-*b*-P(3HT-*alt*-P)**). RHC was chosen above regular differential scanning calorimetry (DSC) because of its increased sensitivity to thermal transitions as a result of the fast scanning rates and the low sample amounts required.[38] The results of the RHC measurements are shown in Figure 4. The **P3HT** homopolymer shows a melting peak around 228 °C, with a melting enthalpy of 24.4 J/g, as expected for this molar mass range.[39] No clear glass transition temperature of **P3HT** can be detected. The **P(3HT-*alt*-P)** copolymer, on the other hand, shows no melting at all and a clear glass transition temperature (T_g) around 122 °C (see also Figure S13, Supporting Information), suggesting that the alternating copolymer is completely amorphous. The incorporation of the pyridine moieties apparently impedes efficient packing of the polymer chains in a crystal lattice. Some enthalpic relaxation can be observed on top of the glass transition due to the different heating and cooling rates applied. In the blend of **P(3HT-*alt*-P)** and **P3HT**, the melting peak of **P3HT** is slightly shifted to lower temperature (224 °C), suggesting that the **P3HT** crystals formed in the blend are a bit less stable. The melting enthalpy of the blend is 13.5 J/g, which corresponds to approximately 60% of the melting enthalpy of **P3HT**, in good agreement with the composition of the blend. The T_g of the blend is difficult to determine, but lower than the glass transition of **P(3HT-*alt*-P)** (likely around 112 °C or lower). The block copolymer shows both a

(considerably broadened) melting peak with a maximum at 217 °C and an even lower and also broadened T_g around 70 °C (see also Figure S13, Supporting Information). The melting enthalpy of the block amounts to only 8.5 J/g, definitely lower than 60% of the melting enthalpy of **P3HT**. This lower melting enthalpy, together with the decreased melting temperature and the broad melting trajectory, points out that the **P(3HT-*alt*-P)** block hinders the crystallization of the **P3HT** block to a larger extent than in the blend, resulting in less perfect and less stable crystals. The lower and broader T_g around 70 °C probably indicates the plasticizing (interphase) effect of the **P3HT**-rich domains on the **P(3HT-*alt*-P)**-rich domains in the microphase separated block copolymer. Thermogravimetric analysis (TGA) of the synthesized materials was performed as well. These measurements revealed that the main degradation starts around 350 °C for all polymers (Figure S14, Supporting Information).

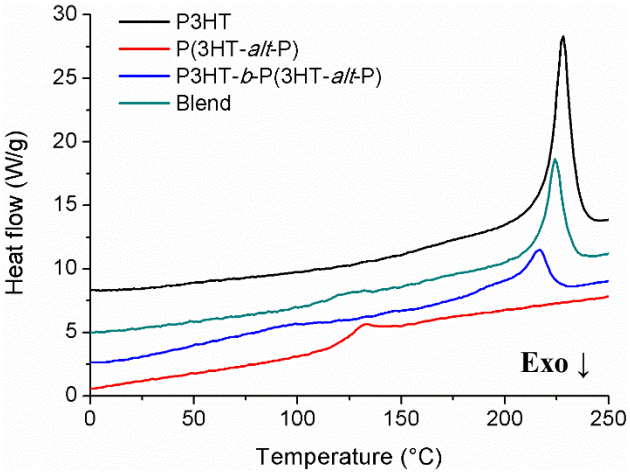

Figure 4. RHC heating profiles, obtained at 500 K/min after cooling at 20 K/min (2nd heating), of **P3HT**, **P(3HT-*alt*-P)**, **P3HT-*b*-P(3HT-*alt*-P)** and the physical blend of **P3HT** and **P(3HT-*alt*-P)** (curves shifted vertically for clarity).

The electrochemical properties of the synthesized materials, of relevance for their possible application in organic electronics, were investigated via cyclic voltammetry. The resulting

voltammograms are depicted in Figure 5. From the overlay of the oxidation scans of all materials (Figure 5a), it is clear that the oxidation characteristics of both **P3HT** and **P(3HT-*alt*-P)** are present in the oxidation profile of the block copolymer and the blend. The oxidation profile of the blend is almost an exact superposition of the voltammograms of the two individual polymer components, with two sharp and nicely separated **P3HT** oxidations and one peak of **P(3HT-*alt*-P)**. In case of the block copolymer, the two oxidation peaks of **P3HT** are less sharp and not so well separated. The reduction characteristics of both constituting polymers are also observed in the reduction profiles of the block copolymer and blend (Figure 5b).

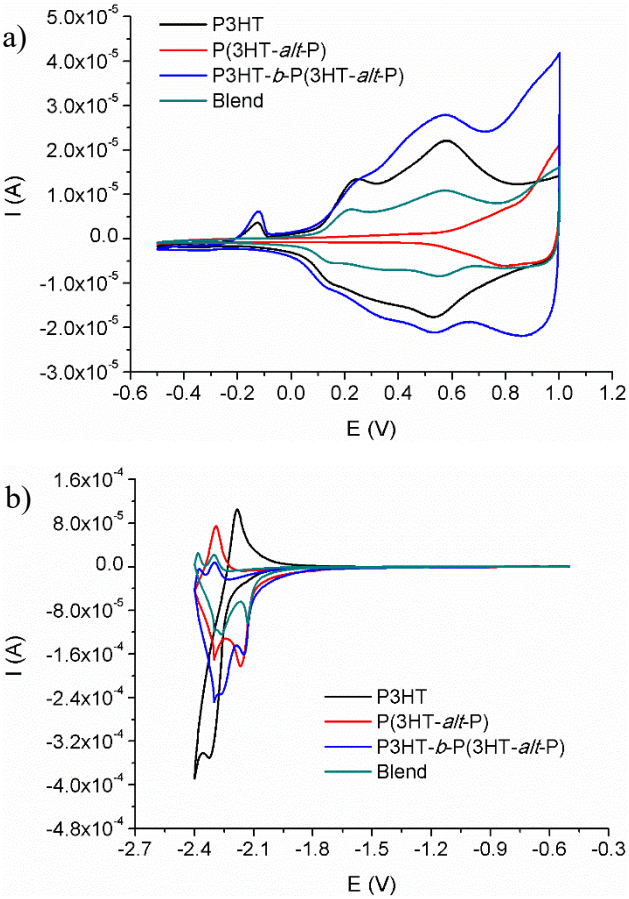

Figure 5. Overlay of the oxidation (a) and reduction (b) scans of **P3HT**, **P(3HT-*alt*-P)**, **P3HT-*b*-P(3HT-*alt*-P)** and the physical blend of **P3HT** and **P(3HT-*alt*-P)** as determined by cyclic voltammetry.

The frontier orbital energy levels of all materials can be obtained from the above voltammograms by determining the onset potentials. The results are presented in Table 2. The HOMO levels (derived from the oxidative onset potentials) of **P3HT**, the block copolymer and the blend are nearly the same, whereas the HOMO of the alternating copolymer lies significantly deeper. The LUMO levels (derived from the reductive onset potentials) of all pyridine-containing polymers are similar, whereas **P3HT** shows a slightly higher LUMO. The largest electrochemical bandgap is observed for the alternating D-A copolymer.

Table 2. Electrochemical properties of **P3HT**, **P(3HT-*alt*-P)**, **P3HT-*b*-P(3HT-*alt*-P)** and the physical blend of **P3HT** and **P(3HT-*alt*-P)** (60/40).

Polymer	$E_{onset,\ ox}$ (V)[a]	HOMO (eV)	$E_{onset,\ red}$ (V)[a]	LUMO (eV)	$E_{g,\ EC}$ (eV)[b]	$E_{g,\ opt}$ (eV)[c]
P3HT	0.12	-5.08	-2.23	-2.73	2.35	2.03
P(3HT-*alt*-P)	0.57	-5.53	-2.10	-2.86	2.67	2.17
P3HT-*b*-P(3HT-*alt*-P)	0.11	-5.07	-2.10	-2.86	2.21	2.06
Blend	0.11	-5.07	-2.09	-2.87	2.20	2.06

[a] Onset potential of anodic/cathodic scan. [b] Electrochemical bandgap. [c] Optical bandgap.

To obtain insight into the optical properties of the synthesized materials and to further prove that indeed a block copolymer was formed, the synthesized polymer materials and the physical blend were also studied by UV-vis and fluorescence spectroscopy. The UV-vis absorption spectra of all materials in solution ($CHCl_3$) are depicted in Figure 6. It is clear that the wavelength at maximal absorbance (λ_{max}) of the block copolymer (424 nm) lies in between those of **P(3HT-*alt*-P)** (413 nm) and **P3HT** (453 nm), whereby the absorbance profile of the block copolymer overlaps with those of the two constituting polymers, but lies more closely toward that of **P(3HT-*alt*-P)**. The absorption spectrum of the blend is quite similar to that of the block copolymer, with the difference that a shoulder is observed in the **P3HT** region and λ_{max} is slightly blue-shifted (422 nm).

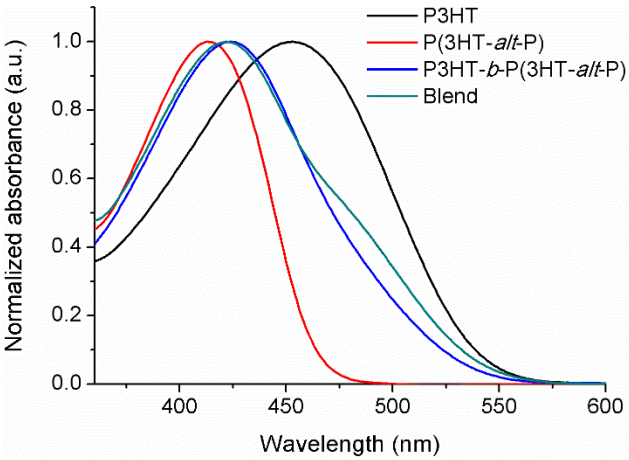

Figure 6. UV-vis absorption spectra of **P3HT**, **P(3HT-*alt*-P)**, **P3HT-*b*-P(3HT-*alt*-P)** and the physical blend of **P3HT** and **P(3HT-*alt*-P)**.

Finally, the fluorescence properties of the polymers were investigated as well. A green-yellow fluorescence was observed for the **P(3HT-*alt*-P)** copolymer, while the **P3HT** homopolymer shows an orange fluorescence and the **P3HT-*b*-P(3HT-*alt*-P)** copolymer a yellow-orange fluorescence (Figure S15, Supporting Information). These visual observations were confirmed by the fluorescence spectra of the materials in $CHCl_3$ solution, which are illustrated in Figure 7. From these spectra it can be determined that the **P(3HT-*alt*-P)** copolymer has an emission maximum at 483 nm, the **P3HT** homopolymer at 582 nm and the **P3HT-*b*-P(3HT-*alt*-P)** copolymer at 563 nm (Table 3). In contrast to the absorption spectra, there is a clear difference between the fluorescence spectrum of the block copolymer and that of the blend. The fluorescence spectrum of the blend (λ_{max} = 483 nm) is mainly determined by the fluorescence spectrum of the **P(3HT-*alt*-P)** copolymer, with only a small contribution from **P3HT**. On the other hand, the fluorescence spectrum of the block copolymer is much broader and definitely not just a superposition of the fluorescence spectra of the two polymer components. This again confirms the successful formation of an all-conjugated block copolymer, which could also

visually be established by means of paper chromatography (Figure S16, Supporting Information).

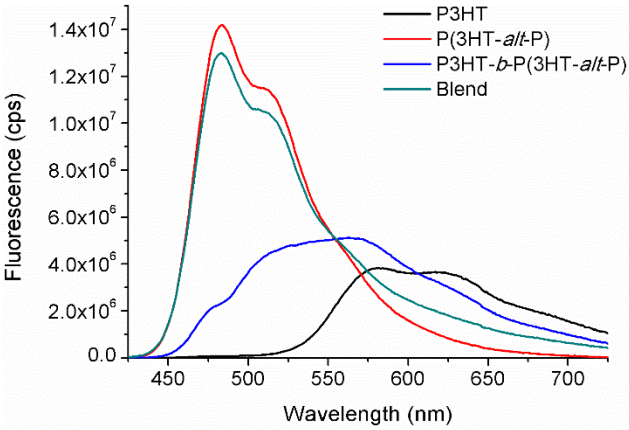

Figure 7. Fluorescence spectra of **P3HT**, **P(3HT-*alt*-P)**, **P3HT-*b*-P(3HT-*alt*-P)** and the physical blend of **P3HT** and **P(3HT-*alt*-P)**.

In addition to the fluorescence spectra, the quantum yields were determined as well (Table 3). A very high quantum yield of 89% was obtained for the **P(3HT-*alt*-P)** copolymer. For **P3HT**, a value of 43% was found, which corresponds to previous literature data.[40] The quantum yield of the block copolymer amounted to 62%, which lies nicely in between the values of the two polymer constituents.

Table 3. Optical properties of **P3HT**, **P(3HT-*alt*-P)** and **P3HT-*b*-P(3HT-*alt*-P)** in $CHCl_3$ solution.

Polymer	Absorbance λ_{max} (nm)	Fluorescence λ_{max} (nm)	Quantum yield (%)
P3HT	453	582	43
P(3HT-*alt*-P)	413	483	89
P3HT-*b*-P(3HT-*alt*-P)	424	563	62

Conclusions

We have shown that an alternating donor-acceptor copolymer (**P(3HT-*alt*-P)**) can be synthesized via Kumada catalyst-transfer polymerization using a nickel catalyst (GRIM polymerization), thereby requiring no toxic tin compounds as is the case for Stille polymerizations. Through several polymerization tests, varying the monomer concentration and the amount of catalyst (separately), it was proven that the KCTP polymerization in this case follows a non-controlled chain-growth mechanism due to dissociation of the nickel catalyst. Nevertheless, rather narrow polydispersities and reasonable molar masses of ~20 000 g/mol could already be obtained after one minute. Moreover, a new all-conjugated block copolymer (**P3HT-*b*-P(3HT-*alt*-P)**) was also successfully formed in a one-pot GRIM procedure by using an *in situ* formed poly(3-hexylthiophene) (**P3HT**) block to initiate the polymerization of the donor-acceptor alternating copolymer as the second block. This was confirmed by GPC and ^{1}H NMR analysis.

The thermal, electrochemical and optical properties of the three polymers and a blend of **P3HT** and **P(3HT-*alt*-P)** were investigated. From the thermal analysis it was clear that the presence of the **P(3HT-*alt*-P)** part in the block copolymer hinders the crystallization of the **P3HT** block. With respect to the optical properties, a clear distinction could be made between the block copolymer and a physical blend of the two polymer components by comparing the fluorescence spectra and quantum yields. The fluorescence spectrum of the block copolymer is not just a superposition of the two polymer parts and definitely differs from the spectrum of the blend, further proving the successful synthesis of the block copolymer. The block copolymer showed a quantum yield of 62%, nicely in between the values for **P3HT** and **P(3HT-*alt*-P)** (43% and 89%, respectively).

The synthesized materials show promising characteristics to be used in organic electronics. The deeper HOMO of the all-conjugated alternating copolymer is for instance an asset in polymer solar cells, as it allows to achieve higher open-circuit voltages.[41] On the other hand, the block copolymer is attractive toward the development of charge-selective interlayers for organic photovoltaics.[42] In this respect, it would be interesting to functionalize the side chains to enable the synthesis of conjugated polyelectrolytes.[43] The high fluorescence quantum yield for the alternating donor-acceptor copolymer renders this material an attractive candidate for sensor and/or bio-imaging applications (for instance in nanoparticle form).[44,45] Efforts in this direction are currently ongoing, while other donor-acceptor combinations will be explored as well.

Associated content

Instrumentation, experimental (synthetic) procedures and characterization data as well as $^{1}H/^{13}C$ NMR, MALDI-TOF, GPC, RHC and TGA figures. This material is available free of charge via the Internet at http://pubs.acs.org.

Author information

Corresponding Author

*E-mail: wouter.maes@uhasselt.be

Acknowledgments

This work was supported by the IAP 7/05 project 'Functional Supramolecular Systems', granted by the Science Policy Office of the Belgian Federal Government (BELSPO). We are also grateful for financial support by the Research Program of the Research Foundation−Flanders (FWO) (project G.0415.14N). S.G. acknowledges Hasselt University for her (BOF) doctoral grant. TA Instruments is acknowledged for the RHC equipment.

References

(1) Shirakawa, H.; Louis, E. J.; MacDiarmid, A. G.; Chiang, C. K.; Heeger, A. J. Synthesis of Electrically Conducting Organic Polymers: Halogen Derivatives of Polyacetylene, $(CH)_x$. *J. Chem. Soc. Chem. Commun.* **1977**, 578–580.

(2) Skotheim, T. A.; Reynolds, J. *Conjugated Polymers: Theory, Synthesis, Properties, and Characterization (Handbook of Conducting Polymers, Third Edition)*; CRC Press, 2006.

(3) Dang, M. T.; Hirsch, L.; Wantz, G. P3HT:PCBM, Best Seller in Polymer Photovoltaic Research. *Adv. Mater.* **2011**, *23*, 3597–3602.

(4) Marrocchi, A.; Lanari, D.; Facchetti, A.; Vaccaro, L. Poly(3-hexylthiophene): Synthetic Methodologies and Properties in Bulk Heterojunction Solar Cells. *Energy Environ. Sci.* **2012**, *5*, 8457–8474.

(5) Ma, W.; Yang, C.; Gong, X.; Lee, K.; Heeger, A. J. Thermally Stable, Efficient Polymer Solar Cells with Nanoscale Control of the Interpenetrating Network Morphology. *Adv. Funct. Mater.* **2005**, *15*, 1617–1622.

(6) Lu, L.; Zheng, T.; Wu, Q.; Schneider, A. M.; Zhao, D.; Yu, L. Recent Advances in Bulk Heterojunction Polymer Solar Cells. *Chem. Rev.* **2015**, *115*, 12666–12731.

(7) Mazzio, K. A.; Luscombe, C. K. The Future of Organic Photovoltaics. *Chem. Soc. Rev.* **2015**, *44*, 78–90.

(8) Xu, S.; Kim, E. H.; Wei, A.; Negishi, E. Pd- and Ni-catalyzed Cross-Coupling Reactions in the Synthesis of Organic Electronic Materials. *Sci. Technol. Adv. Mater.* **2014**, *15*, 044201–044223.

(9) Bao, Z.; Chan, W. K.; Yu, L. Exploration of the Stille Coupling Reaction for the Syntheses of Functional Polymers. *J. Am. Chem. Soc.* **1995**, *117*, 12426–12435.

(10) Suzuki, A. Recent Advances in the Cross-Coupling Reactions of Organoboron Derivatives with Organic Electrophiles, 1995–1998. *J. Organomet. Chem.* **1999**, *576*, 147–168.

(11) Roncali, J.; Leriche, P.; Cravino, A. From One- to Three-Dimensional Organic Semiconductors: In Search of the Organic Silicon? *Adv. Mater.* **2007**, *19*, 2045–2060.

(12) Zhang, Y.; Tajima, K.; Hirota, K.; Hashimoto, K. Synthesis of All-Conjugated Diblock Copolymers by Quasi-Living Polymerization and Observation of Their Microphase Separation. *J. Am. Chem. Soc.* **2008**, *130*, 7812–7813.

(13) Topham, P. D.; Parnell, A. J.; Hiorns, R. C. Block Copolymer Strategies for Solar Cell Technology. *J. Polym. Sci. Part B Polym. Phys.* **2011**, *49*, 1131–1156.

(14) Ouhib, F.; Tomassetti, M.; Manca, J.; Piersimoni, F.; Spoltore, D.; Bertho, S.; Moons, H.; Lazzaroni, R.; Desbief, S.; Jérôme, C.; Detrembleur, C. Thermally Stable Bulk Heterojunction

Solar Cells Based on Cross- Linkable Acrylate-Functionalized Polythiophene Diblock Copolymers. *Macromolecules* **2013**, *46*, 785–795.

(15) Boon, F.; Hergué, N.; Deshayes, G.; Moerman, D.; Desbief, S.; De Winter, J.; Gerbaux, P.; Geerts, Y. H.; Lazzaroni, R.; Dubois, P. Synthesis of Poly[(4,4'-(dihexyl)dithieno(3,2-*b*;2',3'-*d*)- silole)] and Copolymerization with 3-Hexylthiophene: New Semiconducting Materials with Extended Optical Absorption. *Polym. Chem.* **2013**, *4*, 4303–4307.

(16) Lee, Y.; Gomez, E. D. Challenges and Opportunities in the Development of Conjugated Block Copolymers for Photovoltaics. *Macromolecules* **2015**, *48*, 7385–7395.

(17) Wang, J.; Higashihara, T. Synthesis of All-Conjugated Donor–Acceptor Block Copolymers and their Application in All-Polymer Solar Cells. *Polym. Chem.* **2013**, *4*, 5518–5526.

(18) Qiu, Y.; Fortney, A.; Tsai, C.-H.; Baker, M. A.; Gil, R. R.; Kowalewski, T.; Noonan, K. J. T. Synthesis of Polyfuran and Thiophene-Furan Alternating Copolymers Using Catalyst-Transfer Polycondensation. *ACS Macro Lett.* **2016**, *5*, 332–336.

(19) Yokoyama, A.; Miyakoshi, R.; Yokozawa, T. Chain-Growth Polymerization for Poly(3-hexylthiophene) with a Defined Molecular Weight and a Low Polydispersity. *Macromolecules* **2004**, *37*, 1169–1171.

(20) Sheina, E. E.; Liu, J.; Iovu, M. C.; Laird, D. W.; McCullough, R. D. Chain Growth Mechanism for Regioregular Nickel-Initiated Cross-Coupling Polymerizations. *Macromolecules* **2004**, *37*, 3526–3528.

(21) Tkachov, R.; Senkovskyy, V.; Komber, H.; Sommer, J.-U.; Kiriy, A. Random Catalyst Walking along Polymerized Poly(3-hexylthiophene) Chains in Kumada Catalyst-Transfer Polycondensation. *J. Am. Chem. Soc.* **2010**, *132*, 7803–7810.

(22) Geng, Y.; Huang, L.; Wu, S.; Wang, F. Kumada Chain-Growth Polycondensation as a Universal Method for Synthesis of Well-Defined Conjugated Polymers. *Sci. China Chem.* **2010**, *53*, 1620–1633.

(23) Kiriy, A.; Senkovskyy, V.; Sommer, M. Kumada Catalyst-Transfer Polycondensation: Mechanism, Opportunities, and Challenges. *Macromol. Rapid Commun.* **2011**, *32*, 1503–1517.

(24) Nanashima, Y.; Yokoyama, A.; Yokozawa, T. Synthesis of Well-Defined Poly(2-alkoxypyridine-3,5-diyl) via Ni-Catalyst-Transfer Condensation Polymerization. *Macromolecules* **2012**, *45*, 2609–2613.

(25) Palermo, E. F.; McNeil, A. J. Impact of Copolymer Sequence on Solid-State Properties for Random, Gradient and Block Copolymers containing Thiophene and Selenophene. *Macromolecules* **2012**, *45*, 5948–5955.

(26) Willot, P.; Govaerts, S.; Koeckelberghs, G. The Controlled Polymerization of Poly(cyclopentadithiophene)s and Their All-Conjugated Block Copolymers. *Macromolecules* **2013**, *46*, 8888–8895.

(27) Wang, J.; Ueda, M.; Higashihara, T. Synthesis of All-Conjugated Donor−Acceptor−Donor ABA-Type Triblock Copolymers via Kumada Catalyst-Transfer Polycondensation. *ACS Macro Lett.* **2013**, *2*, 506–510.

(28) Bhatt, M. P.; Magurudeniya, H. D.; Sista, P.; Sheina, E. E.; Jeffries-EL, M.; Janesko, B. G.; McCullough, R. D.; Stefan, M. C. Role of the Transition Metal in Grignard Metathesis Polymerization (GRIM) of 3-Hexylthiophene. *J. Mater. Chem. A* **2013**, *1*, 12841–12849.

(29) Magurudeniya, H. D.; Kularatne, R. S.; Rainbolt, E. A.; Bhatt, M. P.; Murphy, J. W.; Sheina, E. E.; Gnade, B. E.; Biewer, M. C.; Stefan, M. C. Benzodithiophene Homopolymers Synthesized by Grignard Metathesis (GRIM) and Stille Coupling Polymerizations. *J. Mater. Chem. A* **2014**, *2*, 8773–8781.

(30) Willot, P.; Moerman, D.; Leclère, P.; Lazzaroni, R.; Baeten, Y.; Van der Auweraer, M.; Koeckelberghs, G. One-Pot Synthesis and Characterization of All-Conjugated Poly(3-alkylthiophene)-*block*-poly(dialkylthieno[3,4-*b*]pyrazine). *Macromolecules* **2014**, *47*, 6671–6678.

(31) Ono, R. J.; Kang, S.; Bielawski, C. W. Controlled Chain-Growth Kumada Catalyst Transfer Polycondensation of a Conjugated Alternating Copolymer. *Macromolecules* **2012**, *45*, 2321–2326.

(32) Nanashima, Y.; Shibata, R.; Miyakoshi, R.; Yokoyama, A.; Yokozawa, T. Investigation of Catalyst-Transfer Condensation Polymerization for the Synthesis of *n*-Type π-Conjugated Polymer, Poly(2-dioxaalkylpyridine-3,6-diyl). *J. Polym. Sci. Part A Polym. Chem.* **2012**, *50*, 3628–3640.

(33) Qiu, J.; Charleux, B.; Matyjaszewski, K. Progress in Controlled/Living Polymerization in Aqueous Media. *Polimery* **2001**, *46*, 453–460.

(34) Yokozawa, T.; Nanashima, Y.; Ohta, Y. Precision Synthesis of *n*-Type π-Conjugated Polymers in Catalyst-Transfer Condensation Polymerization. *ACS Macro Lett.* **2012**, *1*, 862–866.

(35) Miyakoshi, R.; Yokoyama, A.; Yokozawa, T. Catalyst-Transfer Polycondensation. Mechanism of Ni-Catalyzed Chain-Growth Polymerization Leading to Well-Defined Poly(3-hexylthiophene). *J. Am. Chem. Soc.* **2005**, *127*, 17542–17547.

(36) Liu, J.; Loewe, R. S.; McCullough, R. D. Employing MALDI-MS on Poly(alkylthiophenes): Analysis of Molecular Weights, Molecular Weight Distributions, End-Group Structures, and End-Group Modifications. *Macromolecules* **1999**, *32*, 5777–5785.

(37) Iovu, M. C.; Sheina, E. E.; Gil, R. R.; McCullough, R. D. Experimental Evidence for the Quasi-"Living" Nature of the Grignard Metathesis Method for the Synthesis of Regioregular Poly(3-alkylthiophenes). *Macromolecules* **2005**, *38*, 8649–8656.

(38) Wouters, S.; Demir, F.; Beenaerts, L.; Van Assche, G. Calibration and Performance of a Fast-Scanning DSC–Project RHC. *Thermochim. Acta* **2012**, *530*, 64–72.

(39) Spoltore, D.; Vangerven, T.; Verstappen, P.; Piersimoni, F.; Bertho, S.; Vandewal, K.; Van den Brande, N.; Defour, M.; Van Mele, B.; De Sio, A.; Parisi, J.; Lutsen, L.; Vanderzande, D.; Maes, W.; Manca, J. V. Effect of Molecular Weight on Morphology and Photovoltaic Properties in P3HT:PCBM Solar Cells. *Org. Electron.* **2015**, *21*, 160–170.

(40) Li, Y.; Vamvounis, G.; Holdcroft, S. Tuning Optical Properties and Enhancing Solid-State Emission of Poly(thiophene)s by Molecular Control: A Postfunctionalization Approach. *Macromolecules* **2002**, *35*, 6900–6906.

(41) Zhou, H.; Yang, L.; You, W. Rational Design of High Performance Conjugated Polymers for Organic Solar Cells. *Macromolecules* **2012**, *45*, 607–632.

(42) Kesters, J.; Govaerts, S.; Pirotte, G.; Drijkoningen, J.; Chevrier, M.; Van den Brande, N.; Liu, X.; Fahlman, M.; Van Mele, B.; Lutsen, L.; Vanderzande, D.; Manca, J.; Clément, S.; Von Hauff, E.; Maes, W. High-Permittivity Conjugated Polyelectrolyte Interlayers for High-Performance Bulk Heterojunction Organic Solar Cells. *ACS Appl. Mater. Interfaces* **2016**, *8*, 6309–6314.

(43) Ghoos, T.; Van Den Brande, N.; Defour, M.; Brassinne, J.; Fustin, C.-A.; Gohy, J.-F.; Hoeppener, S.; Schubert, U. S.; Vanormelingen, W.; Lutsen, L.; Vanderzande, D. J.; Van Mele, B.; Maes, W. Amphiphilic *N*-Methylimidazole-Functionalized Diblock Copolythiophenes for Organic Photovoltaics. *Eur. Polym. J.* **2014**, *53*, 206–214.

(44) Ethirajan, A.; D'Olieslaeger, L.; Vandenbergh, J.; Lutsen, L.; D'Olieslaeger, M.; Vanderzande, D.; Junkers, T. Synthesis of MDMO-PPV Nanoparticles Via In Situ Sulfinyl Precursor Route Polymerization in Miniemulsion. *Macromol. Chem. Phys.* **2013**, *214*, 1859–1864.

(45) Huynh, T.-P.; Sharma, P. S.; Sosnowska, M.; D'Souza, F.; Kutner, W. Functionalized Polythiophenes: Recognition Materials for Chemosensors and Biosensors of Superior Sensitivity, Selectivity, and Detectability. *Prog. Polym. Sci.* **2015**, *47*, 1–25.

For Table of Contents use only

Synthesis of highly fluorescent all-conjugated alternating donor-acceptor (block) copolymers via GRIM polymerization

Sanne Govaerts,[†] Pieter Verstappen,[†] Huguette Penxten,[†] Maxime Defour,[‡] Bruno Van Mele,[‡] Laurence Lutsen,[§] Dirk Vanderzande,[†,§] Wouter Maes[*,†,§]*

[†] Design & Synthesis of Organic Semiconductors (DSOS), Institute for Materials Research (IMO), Hasselt University, Agoralaan 1 – Building D, B-3590 Diepenbeek (Belgium)

[‡] Physical Chemistry and Polymer Science (FYSC), Vrije Universiteit Brussel (VUB), Pleinlaan 2, B-1050 Brussels (Belgium)

[§] IMOMEC Division, IMEC, Wetenschapspark 1, B-3590 Diepenbeek (Belgium)